A Robust and Automatic Algorithm for TLS–ALS Point Cloud Registration in Forest Environments Based on Tree Locations

Fariborz Ghorbani, Yi-Chen Chen, Markus Hollaus, and Norbert Pfeifer

***Abstract*—Fusing of terrestrial laser scanning (TLS) and airborne laser scanning (ALS) point cloud data has been recognized as an effective approach in forest studies. In this regard, co-registration of point clouds is considered one of the crucial steps in the integration process. Co-registering point clouds in forest environments faces various challenges, including unstable features, extensive occlusions, different viewpoints, and differences in point cloud densities. To address these intricate challenges, this study introduces an automated and robust method for co-registering TLS and ALS point clouds based on the correspondence of individual tree locations in forest environments. Initially, the positions of individual trees in both TLS and ALS data are extracted. Then, a filtering approach is applied to eliminate positions with low potential for corresponding matches in the TLS and ALS dataset. Since larger trees in the TLS data have a higher potential for corresponding matches in the ALS data, an iterative process is applied to identify correspondences between trees in both datasets. After estimating transformation parameters, the co-registration process is executed. The proposed method is applied on six datasets with varying forest complexities. The results demonstrate a high success rate up to 100% if the starting position of the TLS plots are located within ∼4 hectares (∼2000 trees). Additionally, the potential of the proposed method for co-registering TLS data with ALS data across different search areas and varying number of trees is evaluated in detail. The outcomes indicate that successful co-registration of TLS plot with 50 m diameter to ALS data is successful in the best case within a search radius of approximately 113 hectares (∼60,000 tree locations) and in the worst case for around 20 hectares (∼10,000 tree locations) depending on the forest complexity.**

***Index Terms*—Forest, individual tree locations, iterative, point cloud fusion, point clouds, reducing dependency, terrestrial laser scanning (TLS)–airborne laser scanning (ALS) registration.**

I. Introduction

As THE proliferation of remote sensing continues, there is a growing demand for fusing point cloud data collected from various sensors, platforms, and time frames. In this context, point cloud registration plays a crucial role in integrating such data. The main objective of point cloud registration is to find an appropriate spatial transformation to establish correspondence and alignment between two or more sets of three-dimensional (3-D) point clouds. Point cloud registration has a significant role in various applications, including 3-D modeling [1], 3-D change detection [2], object detection [3], robotics [4], and semantic interpretations of 3-D scenes [5]. A highly significant application of point cloud registration lies in inventorying forest patches, in which structural variables of forests, such as tree positions, tree height, basal area, or stem density, are estimated in a large sample area by analyzing the point cloud data. Among the LiDAR systems, airborne laser scanners (ALS) and terrestrial laser scanners (TLS) are widely employed in the field of forest management due to their significant capabilities for characterizing forest environments in 3-D [6].

TLS devices are ground-based statically mounted instruments that emit laser beams and measure the time it takes for the laser pulses to return after hitting objects in the forest environment. This enables the generation of highly accurate and detailed point cloud data of the forest structure from various viewpoints. TLS devices are particularly effective in capturing fine-scale details of individual trees, including their shape, size, branching patterns, and foliage density. They are commonly used in close-range forest surveys and provide clear, accurate, and rapid information about the structural attributes beneath the forest canopy, such as diameter at breast height (DBH) [7]. However, obtaining information about the upper canopy using TLS can be challenging due to occlusion issue and also, it is often difficult to get precise GPS signal in the forest and therefore the positional accuracy of the TLS data is limited [8]. ALS, mounted on manned or unmanned aircraft or helicopters, allows for rapid coverage of large forested areas. It captures laser pulses that penetrate the canopy and measure the time it takes for the reflected pulses to return. This enables the generation of dense point cloud data, which can be used to extract various forest attributes, including canopy height, tree density, and vegetation structure. While ALS provides valuable information about the upper canopy, its ability to capture detailed information about the understory remains somewhat limited. The dense foliage and the complex structure of the understory vegetation pose challenges in accurately detecting and characterizing the vegetation beneath the canopy. The penetration of laser pulses through the upper canopy and the visibility of the understory is dependent on the

Manuscript received 19 September 2023; revised 17 December 2023; accepted 9 January 2024. Date of publication 17 January 2024; date of current version 5 February 2024. *(Corresponding author: Fariborz Ghorbani.)*

Fariborz Ghorbani is with the Department of Photogrammetry and Remote Sensing, Geomatics Engineering Faculty, K. N. Toosi University of Technology, Tehran 15433-19967, Iran, and also with the Department of Geodesy and Geoinformation, Technische Universität Wien, 1040 Vienna, Austria (e-mail: f_ghorbani95@yahoo.com).

Yi-Chen Chen, Markus Hollaus, and Norbert Pfeifer are with the Department of Geodesy and Geoinformation, Technische Universität Wien, 1040 Vienna, Austria (e-mail: yi-chen.chen@geo.tuwien.ac.at; markus.hollaus@geo.tuwien.ac.at; norbert.pfeifer@geo.tuwien.ac.at).

Digital Object Identifier 10.1109/JSTARS.2024.3355173

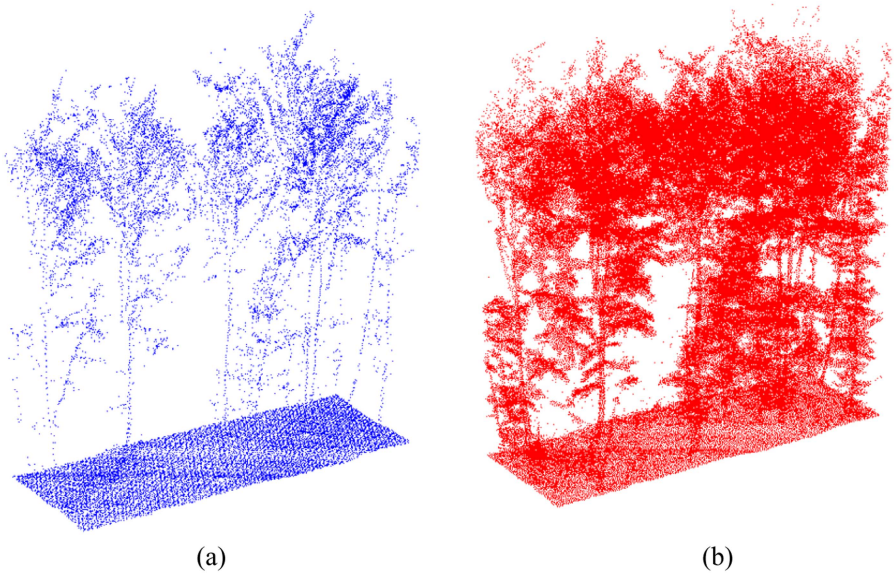

Fig. 1. Visualization of the difference between two-point cloud datasets, ALS (blue) and TLS (red).

density and properties of the vegetation, the used ALS sensor and the acquisition settings, leading to variations in data quality. Fig. 1 demonstrates the density difference between TLS and ALS data and their occlusions.

By integrating ALS and TLS data, the strengths of both technologies can be leveraged to overcome their respective limitations and provide a more comprehensive understanding of forest structure and dynamics. ALS excels in capturing the upper canopy, providing a broad-scale perspective of the forest and getting accurate georeferenced data (in different projected coordinate systems), while TLS is highly effective in capturing fine-scale details of the lower canopy and individual tree attributes. Point cloud registration is therefore one of the most important steps in TLS–ALS data integration.

There are three common frameworks for point clouds registration, which include auxiliary-based, point-based, and feature-based methods [9]. Despite the extensive use of such methods, numerous challenges exist in forested environments, which still hinder the accurate registration of ALS and TLS point clouds. On the other hand, combined approaches have been proposed to address these registration issues by utilizing tree positions as additional data in forested areas [10], [11], [12], [13], [14], [15]. These methods heavily rely on the effective detection of tree positions. When dealing with data from both ALS and TLS platforms in complex forested environments, accurately determining individual tree locations becomes challenging. One reason for it is that ALS and TLS have different viewpoints and thus the detected tree position can differ, e.g., in ALS often the tree top and in TLS the stem position near the terrain is used as tree position. Therefore, this article aims to present an automatic and robust combined approach for ALS and TLS point clouds registration in complex forested environments and reducing the dependency on the accuracy of individual tree locations during the point clouds registration.

A. *Related Work*

The auxiliary-based registration methods commonly utilize global navigation satellite systems (GNSS, e.g., GPS), artificial targets, or color images [16], [17], [18], [19], [20]. Point cloud registration based on GNSS relies on the consistency of GNSS reference coordinates in the two-point cloud datasets. However, in densely forested areas, the GNSS signals are often weak and noisy due to severe obstruction, which poses challenges in obtaining accurate coordinates with TLS. Therefore, this method is not suitable for densely vegetated forest areas. The artificial-target-based approach involves manually placing targets within the study area and using them for registration. While this method has advantages for sparser forest areas, it may not be suitable for densely vegetated natural forests with complex plant growth and high canopy cover. ALS platforms may not accurately measure target positions in natural forests, resulting in improper registration. In addition, placing and maintaining targets in the field for an airborne and a terrestrial survey mission involves additional manual effort and consider more or less simultaneous data acquisitions. Color information provided by cameras [19] can be used as other auxiliary data, but obtaining color images may be time-consuming and the different viewpoints make the identification of corresponding image features a complicated task. The second group of *point-based registration* methods use a direct method that calculates the transformation model between two-point cloud datasets. The iterative closest point (ICP) algorithm is one of the widely used methods in this category [21], [22]. It requires that the same surfaces (or at least surface patches) are mapped in the different point clouds. In addition, the ICP algorithm requires initial estimates of the transformation parameters to the registration process. If the two-point clouds are not close to each other, the ICP algorithm may converge to a local minimum. The forest point cloud data obtained from ALS and TLS are significantly different, making achieving good initial

alignment conditions challenging. Therefore, the initial coregistration in forest environments is usually performed by manually selecting approximate tie points, which is time-consuming and therefore costly. The third group of *feature-based methods* work similarly to target-based methods, using points, lines, or polygons to coregister point clouds. However, these features (such as building corners, vegetation elements, roads, and traffic signs) are automatically identified within the LiDAR point clouds using a feature detector and descriptor [23]. Several methods have been proposed for detecting 3-D keypoints in point clouds, such as SIFT [24], local surface patches [25], intrinsic shape signatures [26], histogram of normal orientations [27], and uniform and competency-based 3-D keypoint detector [28]. In addition to the aforementioned keypoint detection methods, 3-D descriptors, such as FPFH [29], SHOT [30], ROPS [31], binary shape context [32], and 3-D DAISY [33], are used to describe these keypoints and are utilized in the process of matching. On the other hand, some methods extract linear features [34], [35], [36] or planar features [37], [38], [39] as features from point clouds and use them in the process of registration. In this type of method, the transformation is computed by the matched features and this may be used in voting schemes like RANSAC. Feature-based methods are widely used in indoor and urban environments where regular features can be easily identified. Forest environments exhibit a higher complexity and irregularity level than indoor and urban environments. The geometric features of trees and structures within the forest are not easily discernible, making it challenging to utilize explicit geometric features for data registration.

Recently, combined approaches for registration of point clouds in the forest have been proposed to address the lack of reference features in this environment. Tree stems are one of the most stable structures in forest environments. Therefore, current methods for point cloud registration in forest environments have been developed based on extracting information from tree stems. These methods often consist of two steps: tree stem mapping and stem correspondence finding. In the tree stem mapping step, the spatial positions of tree stems and the information on individual tree features, such as tree DBH and tree height, are determined. In the second step, correspondences between tree locations in the two-point clouds are identified using the spatial positions of trees and the extracted features. For example, Henning and Radtke [10] developed a method for tree detection in range images. In this method, the centers of trees are estimated at multiple heights, and the directions of these positions are used for registering the range images. Liang and Hyyppä [11] proposed a method to register TLS point clouds based on tree positions. Each pair of tree positions is compared in this method, and not much attempt has been made to reduce the computational cost. Liu et al. [12] presented an automatic method for stem mapping in different scans of TLS data. This method estimates transformation parameters in 3-D space using stem curvature features at different heights. Kelbe et al. [13] extracted stem maps from TLS data and estimated the 3-D transformation parameters using the spatial locations of the stems in 3-D space and DBH. In their article, nonmatching triplets of stems were eliminated by evaluating the similarity between DBH features and features derived from applying principle component analysis (PCA) to the set of three location points. Tremblay and Béland [40] proposed an extension of the Kelbe et al. [13] method to improve the speed of stem mapping. Instead of using geometric features derived from PCA, they compared the lengths of stems in a triangle of stem locations and the trunk diameter at a horizontal height to measure the similarity between stems. This approach is faster than Kelbe et al. (2016). Dai et al. [41] proposed a method to enhance the speed of TLS point cloud registration in forest environments. This article extracted keypoints using a mode-based analysis of canopy density and the mean shift algorithm. Then, an initial alignment was performed by aligning the keypoints. In the second step, stem locations were identified in each scan, and their overlaps with the initial alignment were refined. The final transformation was computed using the selected stems from the overlapping regions in the scans. This approach aimed to improve the efficiency of point cloud registration in forested areas.

While these methods have been developed for point cloud registration in forest environments, they primarily emphasize addressing the limitations and characteristics of small-scale forest environments, focusing on TLS point clouds. They are not primarily designed for coregistering point clouds obtained from aerial and terrestrial platforms. Recently, methods have been proposed that focus on registering point clouds obtained from aerial and ground-based platforms. Hauglin et al. [42] proposed a method for registering ALS and TLS data. Their method relies on the initial position of individual trees obtained from GNSS receivers. Subsequently, a search algorithm is used to find the best correspondences for individual trees within the TLS and ALS data. Polewski et al. [14] utilized the tree positions for registering ALS data with ground-based photogrammetric point clouds. In this article, corresponding tree descriptors based on spatial distance are determined after identifying the tree positions in both datasets. Finally, the transformation parameters between the two datasets are estimated. A similar approach is employed by Polewski et al. [43] for coregistering unmanned aerial vehicle (UAV) and backpack laser scanner (BLS) point clouds. Guan et al. [44] proposed an approach for coregistering segmented tree geometry in ALS, BLS, and TLS point clouds. The method used in this article is based on establishing correspondences between angles and areas in triangular irregular networks created between tree locations in forest plots. Fine registration is performed using the ICP algorithm. The accuracy of this method depends on the accurate determination of tree positions, and having complete trees in both scenes is essential for aligning the two-point clouds. However, creating such conditions in real-world data can be challenging. Hyyppä et al. [15] proposed a method based on a 2-D local descriptor for coregistering ALS and handheld laser scanner point clouds. This article constructs a 2-D local descriptor on the structured tree positions. Olofsson and Holmgren [46] proposed a method for coreferencing static (TLS) point clouds and dynamic (ALS) point clouds. They presented a stem diameter weighted linking algorithm and a threshold as quality criteria of coregistration. These two features are combined to a simultaneous location and mapping-based coregistration method. In 2022, Shao et al. [45] proposed a method for coregistering

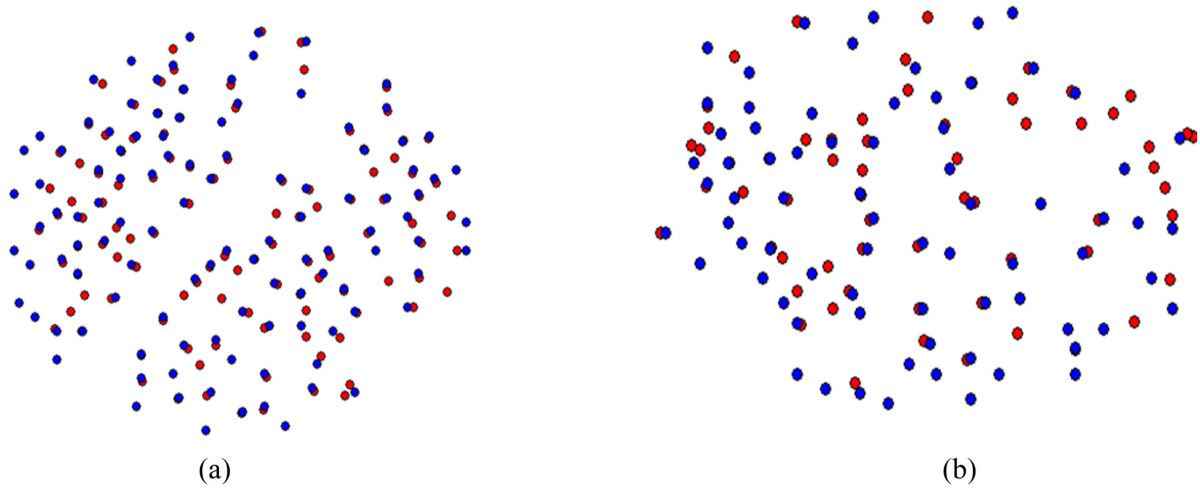

Fig. 2. Illustration of tree positions in two datasets in the same coordinate system acquired with TLS (red points) and ALS (blue points). (a) Location of tree stems with high accuracy and high correspondence level. (b) Location of tree stems with low accuracy and low correspondence level. The patch diameter is around 50 m in both examples.

terrestrial LiDAR (i.e., TLS) and UAV LiDAR data. They first separated ground points from nonground points through filtering, then aligned the ground points of TLS and UAV data. Next, the forest canopy in both datasets was projected onto the aligned ground points, generating a binary canopy image. The canopy edges were extracted using image processing techniques. 2-D keypoints were identified on these edges, and image matching was conducted. Subsequently, the estimated 2-D transformation parameters were utilized for coarse registration. It should be noted that in this method, some information may be lost during the image processing steps, and the dimensions of the study area are limited to the largest plot size of 40 m $\times$ 40 m, which covers a relatively small area. Zhou et al. [47] presented an automatic method to fuse TLS and ALS point clouds using feature points of canopy gap shapes. They initiated the process by extracting the boundaries of canopy gaps and obtaining feature points from the canopy gap vectors using the weighted effective area algorithm. Then, transformation parameters were derived using the coherent point drift algorithm. Finally, the ICP was applied. The method used in this article is implemented in the small plots of point clouds (20 m $\times$ 20 m), and includes a limited number of trees. In addition, the pre-ICP registration accuracy in one of the plots was reported to have an average of approximately 3.5 m.

B. Research Aims

Although position-based tree methods have been continuously advancing, significant limitations still exist. These methods rely on accurately determining tree locations, and achieving high accuracy in tree positioning is crucial for successful coregistration (e.g., [13]). However, these conditions are not always attainable in real-world data. Some of the main reasons for the reduction in the accuracy of tree positioning can be attributed to the different perspectives of data acquisition in ALS and TLS sensors, the applied tree detection algorithms (e.g., local maxima filter based on the CHM for ALS and stem detection based on TLS data), varying levels of detail in point cloud data, high forest density, and complexity of tree growth. Some of these challenges can be seen in Fig. 1.

Fig. 2 illustrates tree positioning in two different datasets, TLS and ALS. The figure depicts the tree locations in two scenarios: an ideal state and a complex state where trees feature patterns deviating from vertical growth. The red points represent the positions of tree stems in the TLS point cloud data, while the blue points indicate the locations of tree tops (and therefore the assumed position of stems) in the ALS point cloud data. The positions of trees were projected on the DTM, resulting in 3-D points at ground height. Fig. 2(a) depicts the tree stem position estimation in both TLS and ALS with appropriate precision. In this image, most of the tree stem positions in TLS have corresponding positions in ALS, and the distances between the corresponding stem positions are minimal. However, Fig. 2(b) represents the positions of trees extracted in a complex forest structure. In this example, a significant percentage of tree stem positions in TLS do not have corresponding location in ALS, and the distances between some corresponding positions are relatively large.

On the other hand, the predominant methods for tree localization are based on tree stem positions obtained from either TLS data in different scans or a combination of UAV and TLS or UAV and MLS data. These data sources cover a limited search radius of the study area. When our goal is to perform registration of ALS and TLS point clouds, we are dealing with a large search radius of the study area in the ALS data. As a result, we encounter diverse complexities in forested regions, and naturally, the accuracy of tree localization will vary. However, the search radius to which the proposed approaches are feasible for implementation in a large area has not been investigated. These factors pose challenges to registering ALS and TLS point clouds.

The main contributions of this article are as follows.

1) Presenting a fully automatic and robust approach for coregistering TLS and ALS point clouds in complex forest environments based on tree localization.

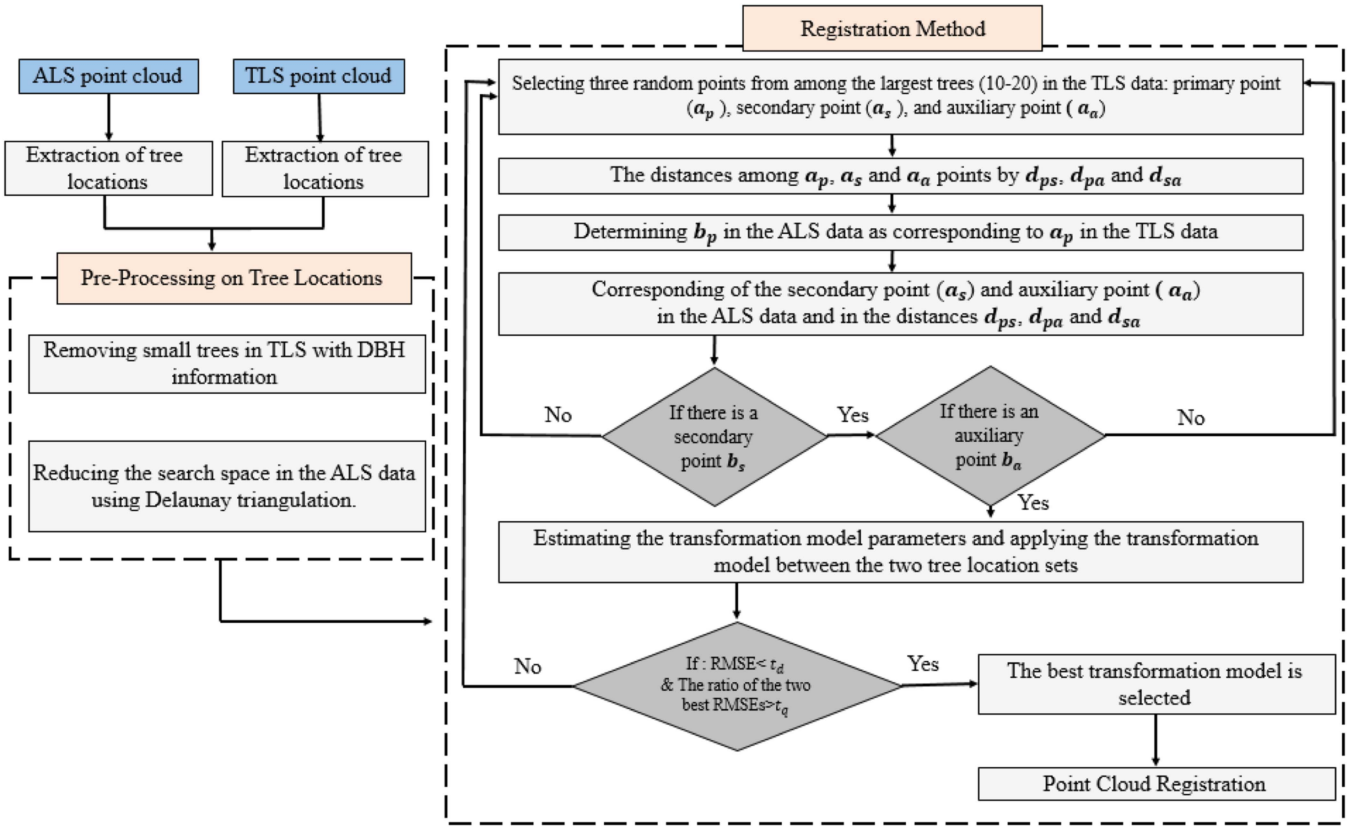

Fig. 3. Overview of registration framework for the TLS and the ALS point clouds.

2) Investigating the performance of the proposed method in point cloud registration for large-area coverage of ALS data and various plots of TLS data.

The rest of this article is organized as follows. In Section II, details of the proposed method are presented. In Section III, the used data are described and the evaluation results of the proposed method are discussed. Finally, Section IV concludes this article.

II. Methods

A. Overview

This article presents an automated and robust approach for registering TLS and ALS point clouds in complex forest environments. The proposed method generally employs an iterative process to find correspondences between the ALS and TLS datasets based on tree locations. Methods that perform registration iteratively are more robust against various types of errors and exhibit good performance in the presence of noise and inaccuracies [48]. This article presents a proposed method that, in addition to registering point clouds in complex forest structures, can also provide high performance in large-scale areas. Fig. 3 shows a flowchart of the proposed method. According to this figure, in the first step, the locations of the trees are extracted in both TLS and ALS data. Then, a preprocessing step is applied to the locations of the extracted trees. Small trees are removed using DBH information in the TLS data at this stage. To identify the corresponding tree locations in both TLS and ALS data, a local triangulations-based approach is adopted to reduce the search space in the ALS data. In the next step, the proposed method is presented for registering the locations of trees during an iterative process. In the following, the details of the proposed method will be presented.

B. Detection of the Individual Tree Locations

Individual tree locations are extracted from both ALS and TLS data. For ALS, individual tree locations are detected in digital surface model (DSM) by a number of local maximum filters, where a kernel size must be determined for each filter beforehand according to the forest composition. Filter results of varying kernel size are then merged and refined by excluding neighbor points within the predefined distance or points having too small DSM height. This step ensures that tree locations represent dominant trees, which are favored for the proposed approach. For TLS, individual tree locations are detected by fitting cylindrical or conical shape, posing a higher possibility of tree stem detection in a scene. This process is widely used for estimating DBH in forestry application. Along with the approximation of tree locations, attribute DBH can be given to each individual tree location to help prioritize starting point selection for the coregistration purpose.

As requirements related to ALS and TLS data, it should be noted that the ground points in these data must be known. Various methods have been proposed to extract ground in forest ALS

point clouds [49], [50], [51] and TLS point clouds [52], [53], [54]. This is due to the fact that tree locations are projected onto terrain surface. Moreover, it is necessary, however, that the data are acquired with the z-coordinate pointing upwards, or equivalently that the direction of gravity is known in both point clouds.

The data processing for tree locations generation was performed via OPALS [55]. OPALS stands for orientation and processing of ALS data, developed by Department of Geodesy and Geoinformation in TU Wien. It provides a complete processing chain for processing ALS data and several fields of application including forestry.

C. Preprocessing of Tree Locations

This section aims to apply an approach that increases the chances of success in the coregistration step. Some trees in the TLS and ALS data are excluded from the processing to enhance the accuracy and speed of the coregistration. Small trees with low height are usually not identified or have high errors in the tree localization methods applied to ALS data. However, in TLS data, the positions of small trees can still be identified. This discrepancy leads to the inability to find corresponding small trees in the ALS data for those extracted in the TLS data. In this article, we applied a preprocessing step to the tree stem locations in TLS. Small trees were removed from the TLS data using DBH information. To achieve this, small trees were identified based on a defined threshold on $\text{SmallTrees} = 0.8 \times \text{Mean}(DBH)$ and subsequently eliminated from the processing pipeline. This threshold was found by empirical analyses.

D. Reducing the Search Space in the ALS Data Using Local Triangulation

To reduce the computational burden in the coregistration step, a stage is incorporated, where, instead of processing the entire ALS data, the focus is on tree locations with a higher potential for identifying correspondence. This idea is inspired by [56], where they used initial matches for global matching. Corresponding triangles between the two sets of triangular structures are utilized to accomplish this. This approach is easily obtained by calculating the edge lengths of triangles in both sets. For this purpose, the 2-D location of the trees in both TLS and ALS data are considered. A local triangulation is performed on both datasets independently using the method [56]. In this method, local triangles are formed by connecting stem positions with k nearest stem positions. In our implementation, we set k to 20 (according to [56]) for ensuring sufficient creation of local triangles to guarantee correspondences between two sets of stem positions. For each triangle in the TLS data, corresponding triangles in the ALS data are identified. Upon verifying each pair of triangles in the TLS and ALS data, the matched pairs of triangles are preserved as the corresponding potential. In contrast, triangles in the ALS data that do not match are filtered out. Initially, the edge lengths in each triangle are sorted in ascending order, and a similarity metric (M_{initial}) between triangles t^T and t^A is determined by applying a threshold on M_{initial} according to the following equation:

$$M_{\text{initial}}\left(t^T, t^A\right) = \sum_{i=1}^{3} \left|L_i^T - L_i^A\right|, \forall \left|L_i^T - L_i^A\right| < dl \quad (1)$$

where L^T and L^A are the lengths of the triangle edges in the TLS and ALS data of tree locations in meter, respectively. dl is a threshold value in meter to consider the correspondence between two triangles. *dl* is considered 1.5 m in this article. The value was derived from practical experimentation, considering the specific accuracy required for this article. Different "*dl*" values could influence the search efficiency in subsequent registration processes. Smaller "*dl*" values might leading to potential errors in the registration. Conversely, higher "*dl*" values might increase computational load without a significant improvement in accuracy. This approach removes edges along the convex hull or from larger forest gaps or clearings. On the other hand, we find the potential corresponding triangles for the TLS data in the ALS data in a way that minimizes the difference between the two triangles. After identifying the initial correspondences, a portion of tree locations that do not have a matched triangular structure is removed. However, there are still a considerable number of outliers among the tree locations, so it is necessary to identify accurate correspondences through a stable process and perform coregistration of the point cloud data. Fig. 4 shows how the search space in ALS data is reduced by the suggested algorithm. In this figure, local triangulations are constructed based on the 2-D positions of the trees (depicted as yellow triangles). For each triangle in the TLS data (represented by a green triangle), the triangles in the ALS data (illustrated as red triangles) that have the potential to be matched are identified. Subsequently, the unmatched tree locations in the ALS data are eliminated. It should be noted that this method does not require additional data.

E. Proposed Method for Point Clouds Registration

The point clouds registration methods need to be robust against various errors and instabilities, which are highly pronounced in complex forest environments. As shown in the flowchart in Fig. 3, the filtered tree locations from TLS and ALS datasets are input into the proposed algorithm. The TLS point cloud is considered as the source and the ALS point cloud as the target. In this method, the 3-D location of the tree location at ground height is being used, where ground height represented by DTM is derived by hierarchical robust interpolation that classifies ALS and TLS data into terrain and off-terrain [49]. We have assumed that larger trees are more likely to be accurately identified in both the TLS and ALS data. The N largest trees from the tree stem locations in the TLS data are selected as reliable points using the information of DBH. In this article, the parameter $N = 15$ indicates the number of chosen tree locations. In the next step, three points are randomly selected from the chosen N tree locations: a primary point (a_p), a secondary point (a_s), and an auxiliary point (a_a). The Euclidean distances among the three points a_p, a_s, and a_a in the 3-D space are calculated as d_{ps},d_{pa}, and d_{sa}, respectively. A point b_{p} in the ALS data is selected as the corresponding point to a_p. In the next step, the

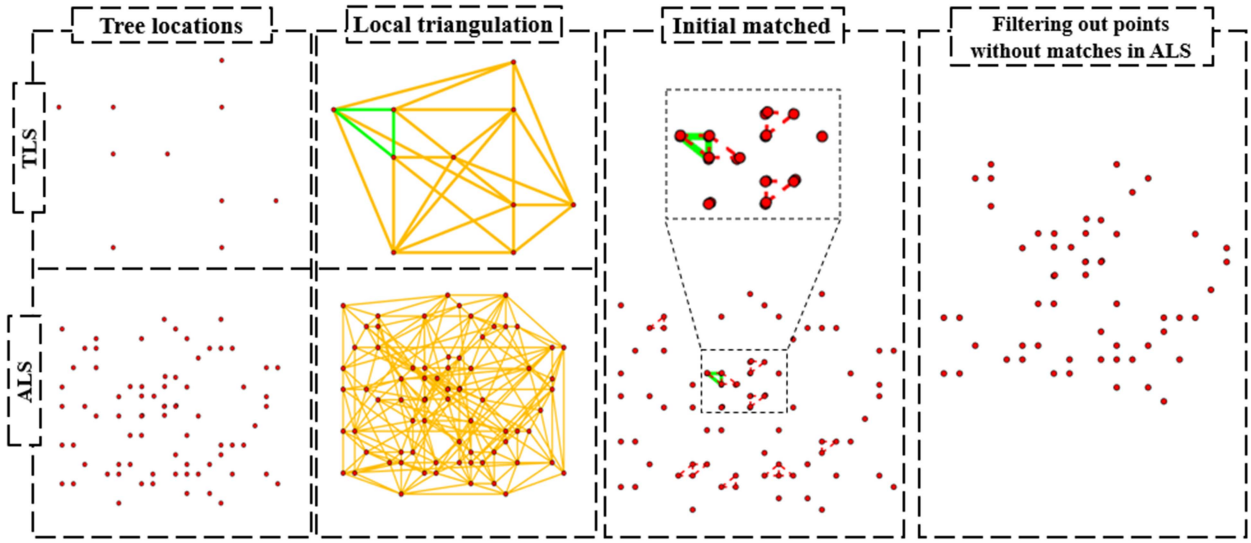

Fig. 4. Illustration of the used approach for reducing the search space in ALS data. In the third column, the green triangle is the correct position of the desired triangle, and the red triangles are the triangles with high similarity potential in the ALS data.

correspondences of points a_s and a_a are searched within the 3-D distances d_{ps} and d_{pa} in the ALS data. Finally, triple points are selected in the ALS data that satisfy the 3-D distances d_{ps}, d_{pa}, and d_{sa} criteria. This process is illustrated in Fig. 5(a)–(d). Fig. 5(a) illustrates three randomly selected points in the TLS data and the calculated lengths between them. In Fig. 5(b), the light blue point represents a randomly selected point in the ALS data, corresponding to the selected point a_p. The search is conducted to find corresponding points a_s and a_a. Fig. 5(c) displays the identified candidates, and the length d_{sa} is checked to determine the edges that match this length. The edges marked with a dashed line do not match d_{sa}. Fig. 5(d) presents the triplets that meet the corresponding conditions. Among them, the corresponding triple 1 is correct, while the corresponding triple 2 is incorrect.

The transformation parameters between the two-point cloud datasets are estimated after selecting candidate correspondences. Then, the best transformation model is used for registration. We consider a scaling factor of 1 in this article since the measurements obtained from TLS and ALS sensors are acquired with known scale. The estimated transformation parameters include three translation parameters and three rotation parameters. The transformation function used is as follows:

$$\begin{bmatrix} X \\ Y \\ Z \end{bmatrix} = R \begin{bmatrix} X' \\ Y' \\ Z' \end{bmatrix} + T \tag{2}$$

where the coordinates *X*, *Y*, and *Z* represent the source point cloud, and *X'*, *Y'*, and *Z'* represent the target point cloud, *T* is the translation vector, and *R* is the rotation matrix.

To select the best transformation model, two decision criteria are used. The first criterion involves applying a threshold on the root mean square error (RMSE) value, and the second criterion consists in using a threshold on the ratio of RMSEs between two tree locations recorded in TLS and ALS data. The calculation of RMSE is as follows:

$$\text{RMSE} = \sqrt{\frac{\sum_{i=1}^{n} \|s_i - t_i\|_2}{n}}. \tag{3}$$

In the equation, *t* is the locations of trees in the target point cloud and *s* represents the locations of trees in the source point cloud after applying the proposed registration method. The distance between the closest locations of the trees is considered after registration, and on the other hand, only one unique nearest distance is considered for each location of the tree. *n* represents the number of corresponding tree locations between the two datasets. For the first criteria, the RMSE value should be lower than a specified threshold (t_d), indicating an acceptable level of alignment between the two datasets. The second criterion for selecting the optimal transformation model is determined by calculating the RMSE for all possible combinations of candidate correspondences in each iteration. The RMSE values are sorted, and the ratio between the two best RMSE values is compared to a specified threshold (t_q). This ratio should exceed the threshold, indicating that the selected transformation model provides a significantly better alignment than other potential models. The reason for using this criterion is to create a unique transformation that is significantly distinct from other transformation models. The following equation expresses this process:

$$Tr_1 = \begin{cases} \text{Selected}, & \text{if } \text{RMSE}(Tr_1) < t_d \ \ \& \ \ \frac{\text{RMSE}(Tr_2)}{\text{RMSE}(Tr_1)} > t_q \\ \text{NotSelected}, & \text{Otherwise} \end{cases} \tag{4}$$

In (4), Tr_1 represents the best transformation model in an iteration. RMSE (Tr_1) and RMSE (Tr_2) denote the RMSE values for the two top-performing transformation models in one iteration. If the above condition is satisfied, the Tr_1 is selected

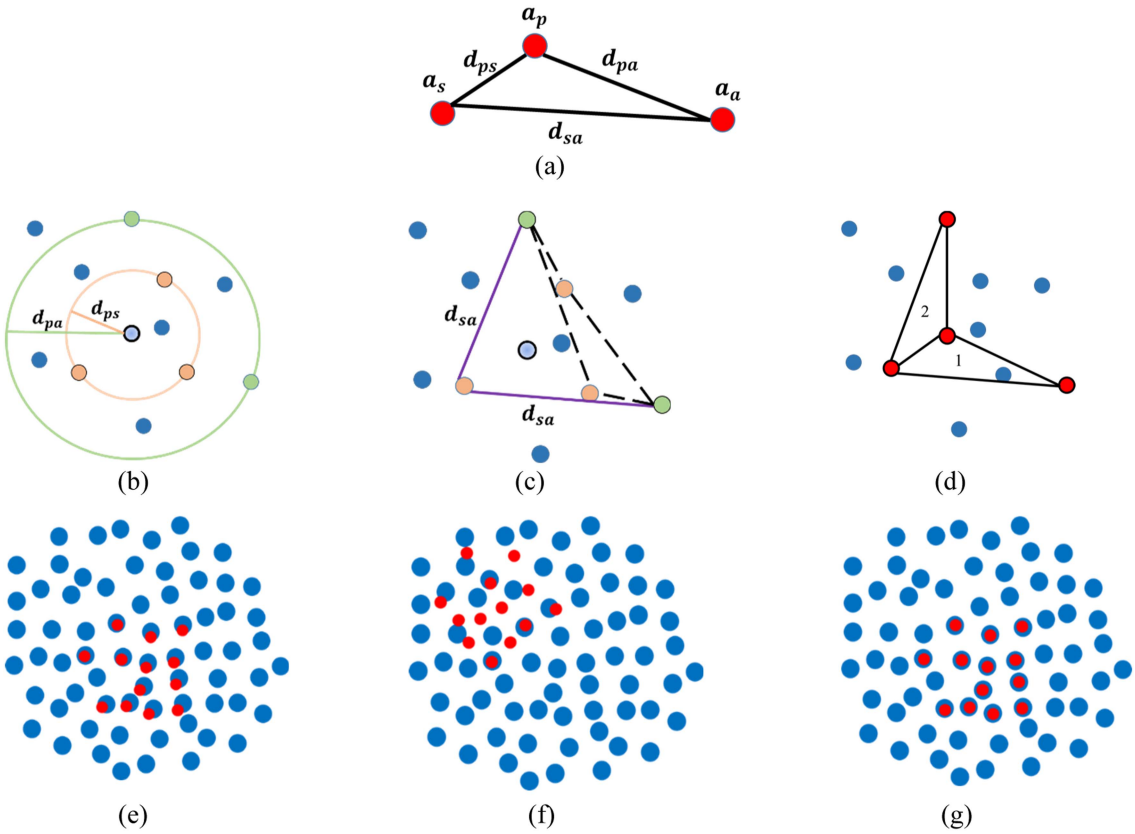

Fig. 5. Process of identifying the best transformation model. (a) Selecting three random points in the TLS data and calculating the Euclidean distances between them. (b) Considering a random point in the ALS data (light blue point) and searching for corresponding points in the d_{ps} and d_{pa} distance. (c) Searching for the third point within the d_{sa} distance in the ALS data. (d) Determining possible corresponding triplets in the ALS data that satisfy the distance constraints. (e) Tree locations after transformation using the correct corresponding triplet. (f) Tree locations after transformation using an incorrect corresponding triplet. (g) True trees position in both.

as the optimal model. In this article, $t_d = 1.2$ m and $t_q = 1.06$ are considered. t_d and t_q were determined based on the specific characteristics and accuracy requirements for tree positioning within the experimental area under investigation. The values were tailored to this particular context, considering the tree density and precision required for this article. However, we want to highlight that our approach involved deriving a set of threshold values tailored for datasets with different characteristics, thereby underlining their adaptability and generalizability across diverse conditions. Fig. 5(e)–(g) show a representation of the registration results between the transformation models obtained from the two corresponding triplets found in the two datasets. According to the figure, when the transformation between two tree locations data is done with correct correspondences [triple 1 in Fig. 5(d)], the RMSE between two-point clouds will be minimum after registration [Fig. 5(e)]. However, when the transformation parameters are derived from incorrect correspondences [triple 2 in Fig. 5(d)], the RMSE after coregistration will be high [Fig. 5(f)]. We utilize this characteristic to iteratively and stably obtain the optimal transformation function for point cloud coregistration.

F. Evaluation Criteria

The proposed coregistration process is evaluated using the metrics of RMSE, root mean square distance (RMSD), and success rate. In order to assess, the actual transformation parameters between the TLS and ALS data are available in all experiments.

The first criterion, RMSE, represents the RMSE value after the final registration. RMSE is calculated according to (3). It quantifies the difference between the coregistered trees position in the TLS and ALS datasets.

The second criterion is RMSD, which is used to assess the accuracy potential of the employed algorithm. This criterion calculates the squared root mean distance between the source point clouds, which have undergone the coregistration algorithm, and their corresponding true positions. If we consider the source point clouds after applying the registration algorithm (s) and their corresponding true positions (g), the RMSD value is calculated as follows:

$$\text{RMSD} = \sqrt{\frac{\sum_{i=0}^{n} \|s_i - g_i\|_2}{n}} \tag{5}$$

where n is the total number of points in the source point cloud.

The third criterion is the success rate that is used to measure the success of the coregistration process. This criterion indicates the proportion of successful coregistration cases and determines the possibility of entering the secondary coregistration stage (e.g., ICP). The success rate is defined as

(a) (b) (c)

Fig. 6. View of plots. (a) Plot A. (b) Plot B. (c) Plot C.

follows:

$$\text{Success rate} = \frac{N_{as}}{N_a} \times 100 \tag{6}$$

where N_{as} is the number of successful registration and N_a is the total number of tests performed. For each test, the initial positions of the TLS and ALS point cloud data differ in both rotation and translation.

III. Results and Analyses

A. Study Area and Data Collection

This article selected the SilviLaser 2021 Benchmark Dataset [57] as test data, which was acquired during the SilviLaser conference 2021 in Vienna. The campaign took place within Vienna Woods in Lower Austria in October 2021. The benchmark aims to demonstrate the different terrestrial system's capabilities for capturing 3-D scenes in various forest conditions. The dataset consists of 1) TLS, MLS, and terrestrial photogrammetric systems contributed by the participants; and 2) ALS and in-situ as reference provided by the organization team. Eight forest plots (plot A1–D2) were installed in the benchmark and six plots (plot A1–C2) are used in this article, where all plots have TLS data scanned by the company RIEGL using a RIEGL VZ-400i. A view of these plots is presented in Fig. 6. Each plot was formed with a 25-m radius circular area and different tree species (i.e., spruce, pine, beech, and white fir), forest structures (i.e., one layer, multilayer, natural regeneration, and deadwood), and age classes (∼50–120 years). With respect to ALS data, the acquisition took place in the end of April 2021. The scanner was RIEGL VQ-1560 II-S and flight height was between 870 and 720 m above ground level. The average point density is 200 pts/m^2 for ALS data and 200 000 pts/m^2 for TLS data. These data align well with the objectives of the article. The dataset includes areas with regularly grown trees and lower complexity, such as Plot A, where it is easily possible to determine the locations. In addition, this dataset comprises areas with irregularly grown trees, high density, and complexity, posing challenges in determining the locations of tree stems, such as Plot B and C.

B. Results of Determining the Locations of Tree Stems

In this section, the results of tree identification in different plots are presented and discussed. Fig. 7 shows the results of locations extracted from tree stems. The size and specifications of the data used in Fig. 7 are presented in Table II. In this figure, the first two columns are point clouds and tree locations in ALS data, respectively, and the third and fourth are point clouds and tree locations in TLS data. The fifth column shows the overlapping region of the tree locations in TLS and ALS data. The blue points indicate tree locations in the ALS data, while the red points represent tree locations in the TLS data. Table I provides the accuracy of matching between ALS and TLS for the extracted tree stem locations. The corresponding tree stem locations for each plot were determined based on their true locations by calculating the Euclidean distance and applying a threshold limit. In this article, trees with distances less than 1.5 m were considered as corresponding tree locations. The RMSE criterion was calculated for the locations of the corresponding trees in each plot using 3.

In addition, the percentage of tree locations without correspondence in the overlapping areas between TLS and ALS data is reported for each dataset (Table I). Based on Fig. 7 and Table I, plot A1 and A2 are classified as good areas, as a majority of points in both TLS and ALS data correspond to each other, with an RMSE of approximately 0.45 m for the corresponding points. However, in plot B, many locations in TLS data do not correspond and RMSE is around 0.75 m. Other characteristics of plot B are the similarity of the neighborhood patterns of trees and a high tree density in the ALS data. On the other hand, plot C exhibits a high percentage of tree locations without correspondence in both ALS and TLS data. Consequently, plot B and plot C can be classified as complex areas.

C. Registration Results of Forest Point Clouds

In this section, we present the registration process results using the proposed method. The algorithm was implemented in MATLAB 2022b on a PC with an AMD FX-8350 processor and 16 GB RAM. The TLS point clouds were considered the source, and the ALS point clouds as the target in this article. To evaluate the performance of the proposed algorithm, the TLS data were transformed using the rotation matrix with angles *Rx*,

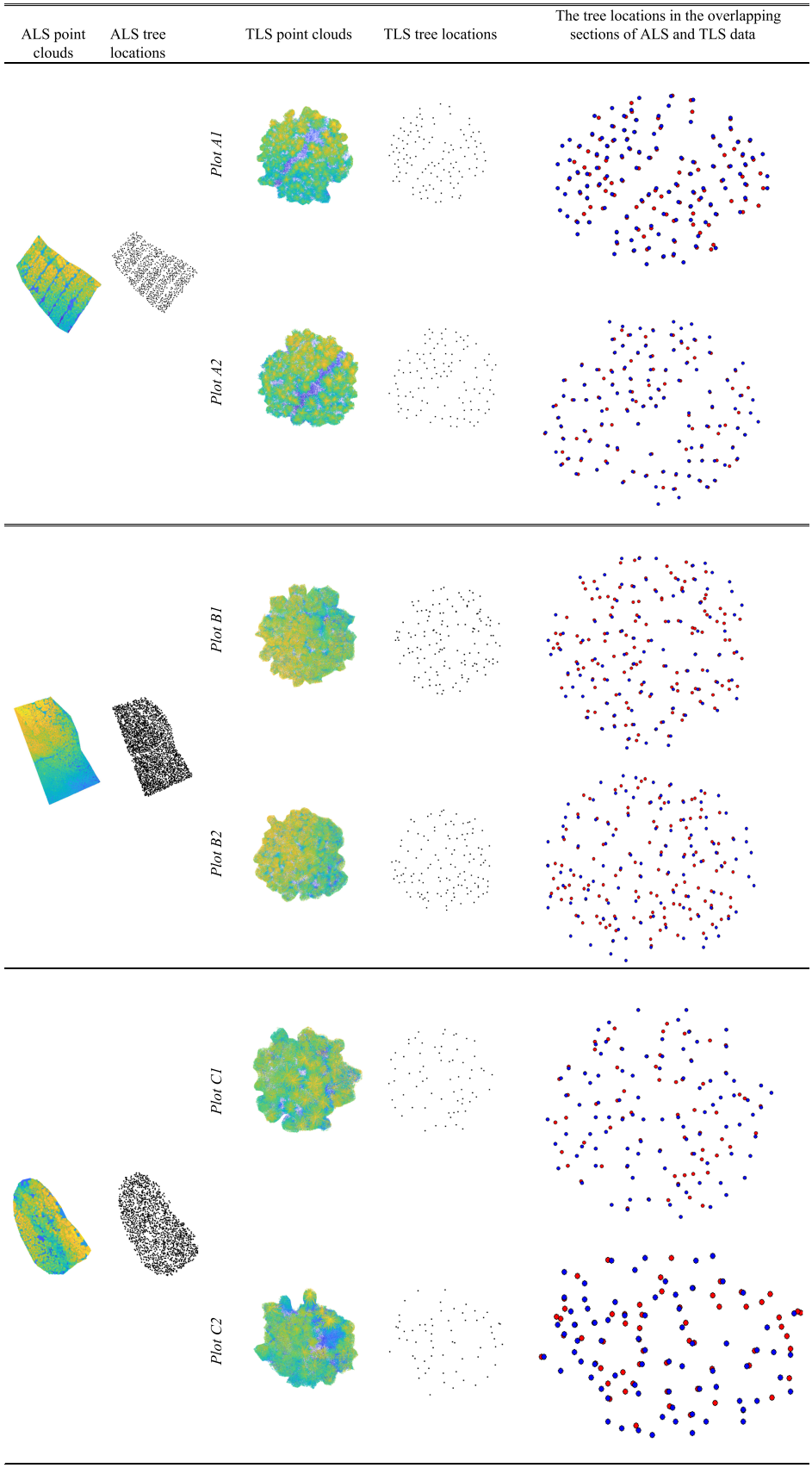

Fig. 7. Visualization of extracted tree locations.

TABLE I
ACCURACY OF EXTRACTED TREE LOCATIONS

Data	Number of tree locations		RMSE (m)	TLS without match %	ALS without match %
	TLS	ALS (in overlap area with TLS)			
Plot A1	113	93	0.45	18	4
Plot A2	103	83	0.44	10	2
Plot B1	135	106	0.75	49	12
Plot B2	121	111	0.80	42	19
Plot C1	67	72	0.70	31	41
Plot C2	63	74	0.69	35	42

TABLE II
ACCURACY RESULTS OF THE PROPOSED METHOD

Data	Area (ha)		Number of tree locations		RMSE (m)		RMSD (m)		Successes rate %
	TLS	ALS	TLS	ALS	Avg	Sd	Avg	Sd	
Plot A1	0.15	2.30	113	841	0.55	0.07	0.38	0.15	100
Plot A2	0.14	2.30	103	841	0.53	0.05	0.31	0.09	100
Plot B1	0.14	4.70	135	2003	0.92	0.15	0.90	0.19	100
Plot B2	0.13	4.70	121	2003	0.94	0.11	0.87	0.20	100
Plot C1	0.14	4.00	67	1404	0.77	0.09	0.53	0.27	100
Plot C2	0.11	4.00	63	1404	0.74	0.21	0.61	0.10	100

Ry, and *Rz* (between [0–360] degree), and the translation vector *tx*, *ty*, and *tz* (between [50–250] m) relative to its true position. These transformations were applied manually, and the resulting positions were considered the initial positions of the TLS and ALS point clouds relative to each other. For each data, 10 initial positions are generated (initial positions are different in terms of both rotation and translation viewpoints) and the coregistration process is repeated 10 times.

Consequently, the true transformation function between the two-point clouds was known and used for evaluating the results of the proposed method. Fig. 8 showcases the results of point cloud registration using the proposed method on different data. The size and specifications of the data used in Fig. 8 are presented in Table II. The figure displays an initial position of the TLS and ALS point clouds, an overview of the point cloud registration, and registration details at two levels. In addition, Table II presents the accuracy results of the proposed method on the TLS and ALS data. The table includes the average RMSE, RMSD (for successful registration), and success rate. The values presented in the table are the outcomes of conducting the coregistration process 10 times for each data, utilizing distinct initial positions encompassing variations in rotation and translation. According to Table II, searching the correct location of the TLS plot within an area of 2–4 ha was successful for all plots and will be discussed in detail in Section III-G.

D. Potential of TLS and ALS Point Cloud Registration in Large Areas

In existing article, there has been a lack of focus on evaluating the effectiveness of registration methods for large areas. Since ALS data cover a significant portion of the ground surface, it is crucial to assess the applicability of the proposed registration method across different spatial search radiuses of ALS data. In this section, we investigate the performance of the proposed method for TLS and ALS point cloud registration within various limits. To conduct this investigation, zones with different radii of ALS data are defined. These zones are centered on the TLS data. Through manual matrix rotation and translation, initial positions are established for TLS and ALS data. Subsequently, the proposed method is employed to perform coregistration between the TLS data and different areas of ALS data.

Fig. 9 showcases the successful registration of tree locations in TLS and ALS data using the proposed method, particularly in the most extensive range of ALS data. In addition, this figure visually represents tree position locations within the overlapping region after registration. The blue points indicate the tree locations in the ALS data, the red points represent the tree locations in the TLS data after applying the proposed registration method, and the green points depict the true tree locations in the TLS data.

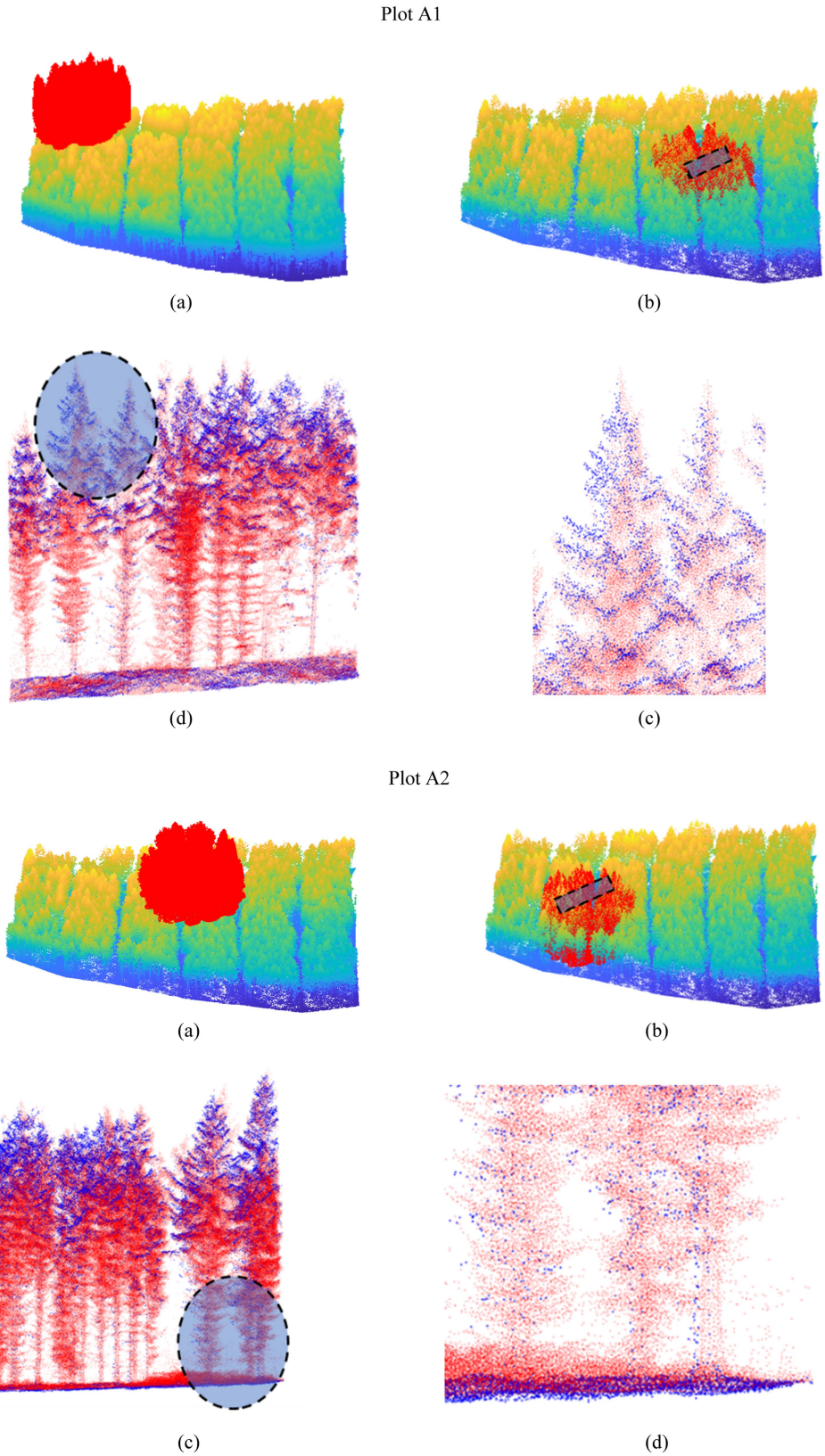

Fig. 8. Point cloud registration results. (a) Initial position of TLS and ALS point clouds. (b) Overview of point clouds registration results. (c) Detailed view of registration results at the first level (indicated by black dashed line in Figure (b). (d) Further detailed view of registration results at the second level (indicated by black dashed line in Figure (c).

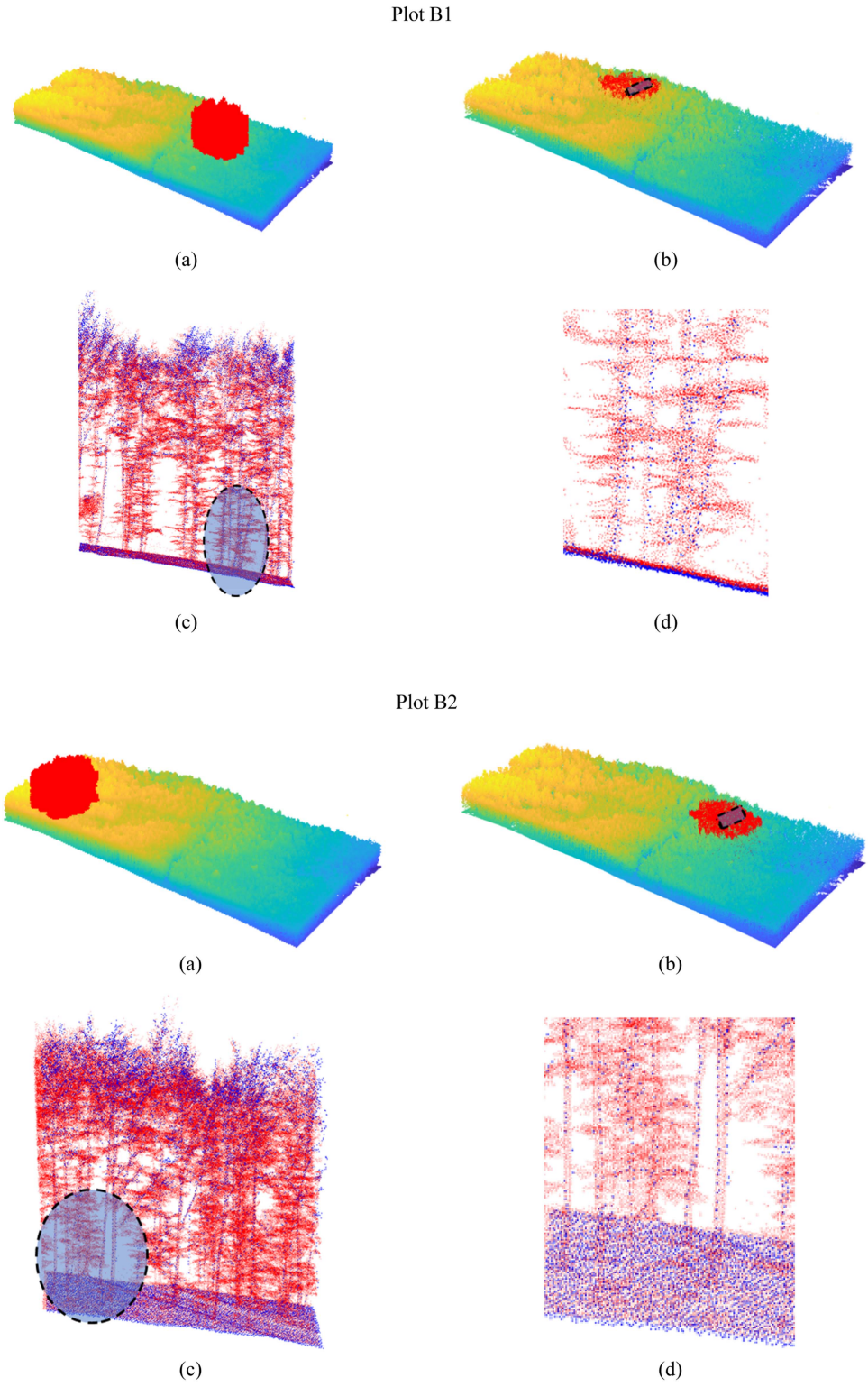

Fig. 8. *(Continued.)*

The results of RMSE and the success rate obtained from the coregistration process for different search radiuses of ALS data are presented in Fig. 10. In this article, 10 experiments were conducted for each radius with various initial positions of the data in terms of rotation and translation. Fig. 10(a) shows the rise in the quantity of tree locations in ALS based on various radii. Fig. 10(b) illustrates the success rate of the proposed method for all radii. According to these results, the proposed method has achieved a 100% success rate up to a radius of approximately 100 m for all data. For data A1 and A2, the success rate reaches

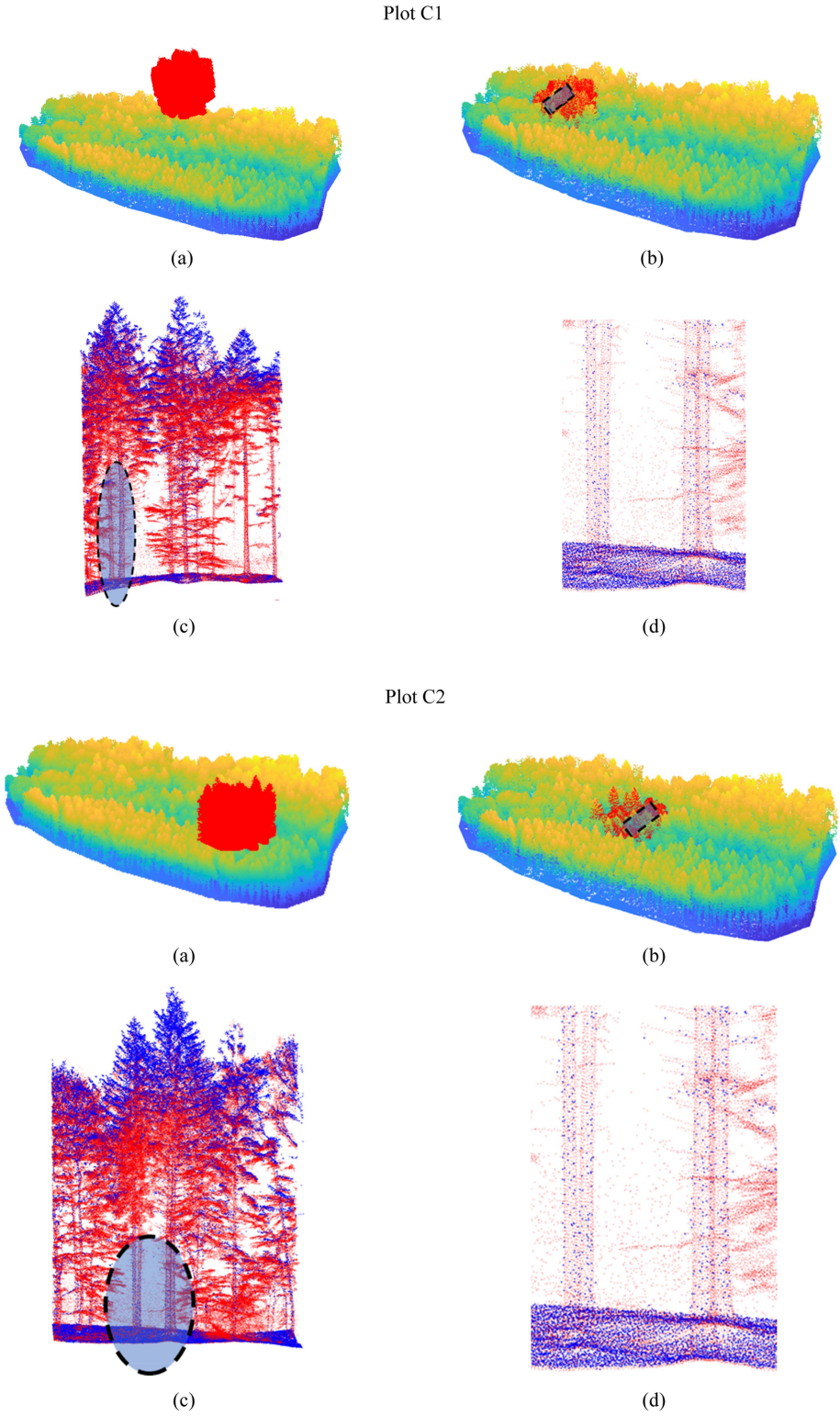

Fig. 8. *(Continued.)*

100% up to radii of 400 and 500 m, respectively, and the coregistration process is successful up to a radius of 600 m with very high success rates (80% and 90%, respectively).

For the other plots, where the localization error of tree stems is higher, the success rate decreases with increasing radius. Nevertheless, the proposed method has managed to successfully perform the coregistration process for plots B1, B2, C1, and C2 up to radii of 300, 300, 350, and 250 m, respectively. The success rates in these radii are above 50%.

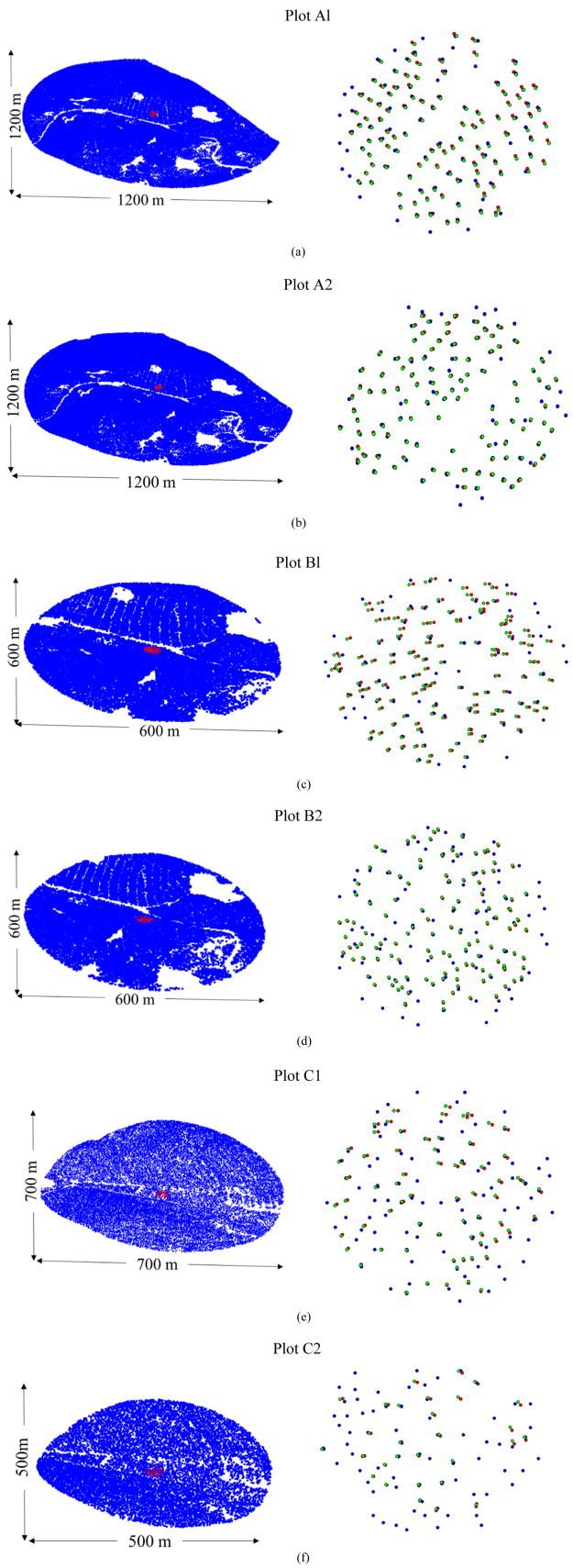

Fig. 9. Successful tree location registration results for the largest range of ALS data.

Fig. 10(c) illustrates the average RMSE outcomes for each radius in experiments where the coregistration process was successful. On the other hand, Table III presents the average RMSD and RMSE metrics for the data with the largest radius where the coregistration process was successful. This table reports the area of the successfully registered region and the number of tree stem positions in that area.

E. Computation Time Performance

This part demonstrates the proposed method's time performance for registering TLS and ALS point clouds. This evaluation assesses the time performance across six plots at various radii. As depicted in Fig. 11, the time performance of the proposed method is presented for the radius where the registration is successfully conducted. In this evaluation, the coregistration process is completed in the shortest time for plot A data and takes the longest in plot B data. For instance, the time performance of the proposed method for a radius of 150 m (covering an approximate 7-ha area) in plots A1, A2, B1, B2, C1, and C2 data are 24, 18, 134, 330, 95, and 98 s, respectively. This value increases with the expansion of the radius of the area.

F. Comparative Performance

This section provides a comparative analysis of the performance of the proposed method for coregistering complex forested TLS and ALS point clouds with the approach presented by Hyyppä [15]. Hyyppä et al. utilized a tree-locations-based approach for coregistering ALS and backpack data. The MATLAB code implementing their method has been made available to users.[1]

The data used in this article (according to Table II) were employed for this evaluation. Table IV displays the results of the performance comparison between these two methods. This assessment demonstrates that the method by Hyyppä et al. [15] successfully operates on the data of plot A, yielding RMSD values of 0.22 and 0.15 m for plot A1 and plot A2, respectively. However, despite its computational efficiency, this method has not provided successful results when faced with the data of plots B and C. In contrast, the proposed method has successfully executed the registration process with appropriate accuracy and reasonable time across all plots. It should be noted that the time performance of the by Hyyppä [15] is better.

G. Comparison of Performance With/Without Removing Small Trees

In this section, a comparison of the proposed method's performance with and without the removal of small trees has been conducted. For this evaluation, all plots used in this article have been utilized. The ALS data were evaluated within areas with a 100-m radius centered on the TLS data positions. All initial conditions for comparison, as outlined in the article's principles, have been met. Table V displays the results of this evaluation for

[1][Online]. Available: https://gitlab.com/fgi_nls/public/2d-registration

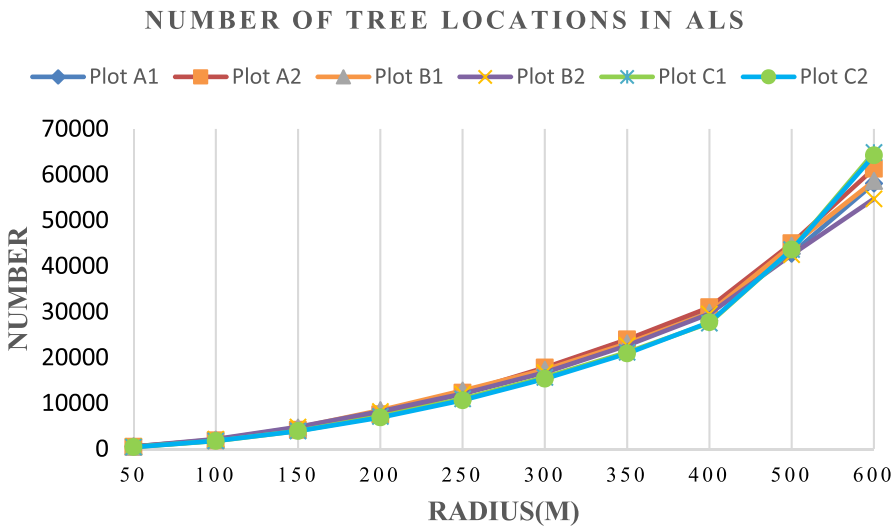

(a)

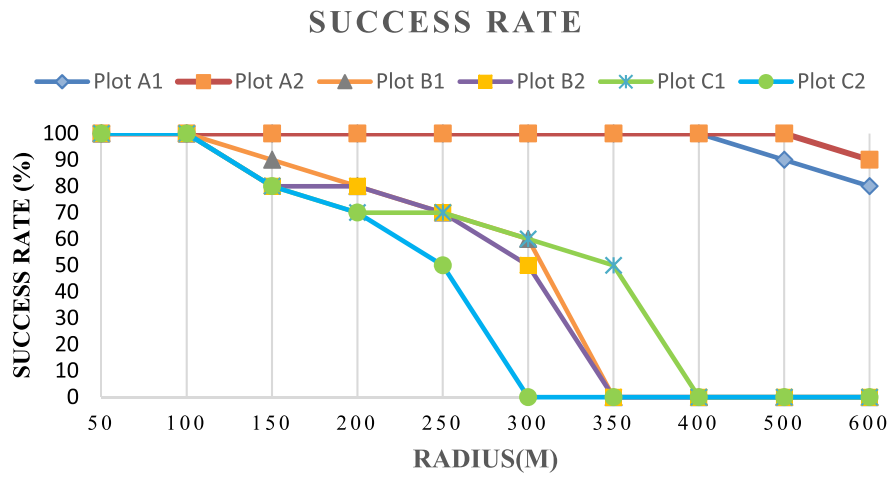

(b)

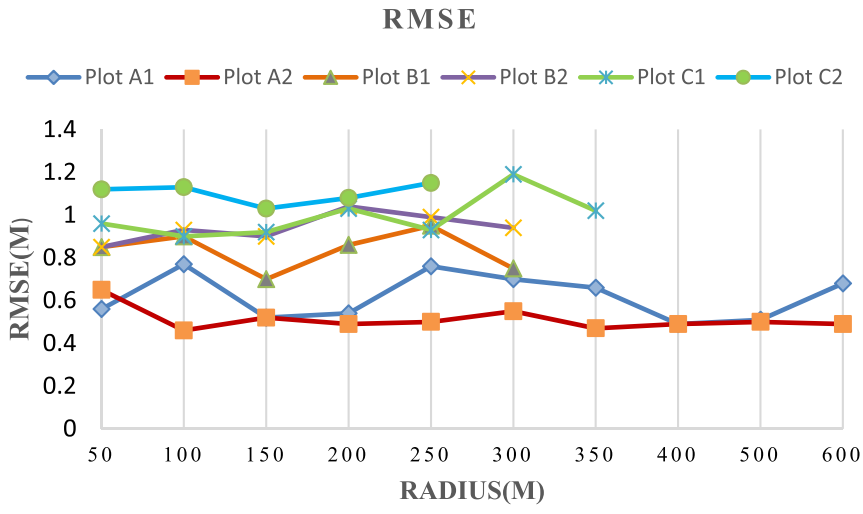

(c)

Fig. 10. Accuracy of registration in different areas of ALS data.

TABLE III
AVERAGE REGISTRATION ACCURACY FOR THE PROPOSED METHOD IN THE DATA WITH LARGE AREAS

Data	Max area (ha)	Number of tree locations in the ALS search area	RMSE (m)		RMSD (m)	
			Avg	Sd	Avg	Sd
Plot A1	113.10	58094	0.62	0.12	0.53	0.19
Plot A2	113.10	61312	0.51	0.05	0.46	0.14
Plot B1	28.27	17314	0.83	0.09	0.86	0.14
Plot B2	28.27	16711	0.94	0.06	0.91	0.15
Plot C1	38.48	19255	0.99	0.10	0.51	0.22
Plot C2	19.63	10657	1.09	0.04	0.65	0.16

Fig. 11. Demonstration of the time performance of the proposed method in different radii.

TABLE IV
COMPARATIVE PERFORMANCE RESULTS

	Hyyppä et al. [15]			Proposed method		
	RMSE (m)	RMSD (m)	Time process (s)	RMSE (m)	RMSD (m)	Time process (s)
Plot A1	0.64	0.22	0.31	0.55	0.38	13
Plot A2	0.51	0.15	0.29	0.53	0.31	16
Plot B1	1.69	64.68	0.89	0.92	0.90	40
Plot B2	1.52	84.26	0.85	0.94	0.87	61
Plot C1	1.63	143.94	0.51	0.77	0.53	27
Plot C2	2.09	110.25	0.49	0.74	0.61	38

TABLE V
PERFORMANCE OF THE PROPOSED METHOD WITH/WITHOUT REMOVING SMALL TREES

Criterias	Data / Method	A1	A2	B1	B2	C1	C2
Time performance (s)	With removing small trees	6	7	40	83	68	55
	Without removing small trees	17	12	772	833	1479	1349
RMSE (m)	With removing small trees	0.77	0.46	0.90	0.93	0.90	1.13
	Without removing small trees	0.87	0.53	1.07	1.11	1.04	1.22
Success rate (%)	With removing small trees	100	100	100	100	100	100
	Without removing small trees	100	100	80	70	100	90

time performance, RMSE, and success rate metrics. According to this table, the running time of the proposed method has significantly decreased, and on the other hand, precision has improved with the removal of small trees.

H. Discussion

The results have shown that the proposed method can effectively perform point cloud registration between the two sensors, TLS and ALS, in forest environments with complex structures (Fig. 8). The details of point cloud registration are also provided at two levels, indicating the satisfactory accuracy of the proposed method. Table II provides quantitative results of point cloud registration accuracy. In this evaluation, the registration process has been iterated 10 times, and for each test, the initial positions of TLS vary in terms of rotation and translation. ALS position was considered fixed. The results indicate that the point cloud registration accuracy is highly accurate, considering the accuracy of trees stem localization. For instance, the RMSE values for plot A1 and plot A2 are 0.55 and 0.53 m, respectively, while the RMSE for trees stem positions in the ground truth is 0.45 and 0.44 m (Table I). The RMSE values for plot B1, plot B2, plot C1, and plot C2 are reported as 0.92, 0.94, 0.77, and 0.74 m, respectively.

On the other hand, the RMSD metric, which represents the difference between the true and registered positions for all TLS data in all plots, was calculated. The RMSD values for plot A1, plot A2, plot B1, plot B2, plot C1, and plot C2 are 0.38, 0.31, 0.90, 0.87, 0.53, and 0.61 m, respectively. The point cloud registration accuracy among different plots indicates that plot A has the highest accuracy, while plot B has the lowest. The lower accuracy of plot B is attributed to errors resulting from trees stem localization, similar patterns of neighboring trees, and high tree density, which make it challenging to find correct correspondences. However, the success rate in all conducted independent experiments for different rotations and translations of the two-point clouds is 100%, irrespective of trees stem localization errors, indicating the proposed method's high stability against various errors in the initial data.

The proposed method was evaluated in regions with different search radiuses of ALS data. The results of coregistering tree positions to the largest possible area are presented in Fig. 9. Fig. 10 shows the results of RMSE and the success rate obtained from the coregistration process for various search radiuses of ALS data. According to this figure, the proposed method achieves a 100% success rate up to approximately 4 ha (containing $\sim$2000 tree locations) for all data. Given the accurate positioning of individual trees in data A1 and A2, the success rate reaches 100% up to radii of 400 and 500 m, respectively. Therefore, the proposed method is capable of performing the coregistration process successfully in an area of approximately 113 ha. The average RMSE values for plot A1 and A2 are 0.62 and 0.51, respectively. Similarly, the average RMSD values for these plots are 0.53 and 0.46 m, respectively.

Moreover, concerning datasets B1 and B2, as illustrated in Table I, a notable proportion of tree locations in the TLS dataset lack corresponding counterparts in the ALS data, and the determined RMSEs of individual tree positions are 0.75 and 0.80 m, respectively. In these plots, the success rate decreases with increasing radius. Nevertheless, the proposed method has been able to perform the registration with a success rate of over 50% for both plots up to an area of approximately 28 ha. Within 28 ha, the average RMSE values for plots B1 and B2 are 0.83 and 0.94 m, respectively. Correspondingly, the average RMSD values for these two plots are 0.86 and 0.91 m, respectively.

For data C plots, as indicated in Table I, the number of identified individual tree positions for plots C1 and C2 is 67 and 63, respectively. This suggests that the number of tree positions in these plots is almost half compared to other plots. In addition, a significant number of tree positions in the ALS data do not have corresponding matches in the TLS data. Despite these characteristics, the proposed method is able to successfully perform the coregistration process for plot C1 up to an area of approximately 38 ha and for plot C2 up to an area of approximately 20 ha, both with a success rate above 50%. The reported RMSE and RMSD values for Plot C1 are 0.99 and 0.51 m, respectively. For Plot C2, the values are 1.09 m for RMSE and 0.65 m for RMSD.

According to Tables II and III, it can be observed that the RMSE and RMSD values for the two conducted experiments do not exhibit significant differences. This is due to the fact that the tree positions in the plots remain consistent in both experiments, with the only difference being the extent of increase in the ALS data in the second experiment. As a result, when the coregistration process is successfully performed, the RMSE and RMSD values are close on average in both tests. The main difference lies in the success rate of the coregistration process, whereas the area increases, the success rate follows a decreasing trend.

The proposed method was compared to a tree-location-based approach [15]. According to Table IV, the method by Hyyppä et al. [15], despite its high computational speed, achieved success only in the coregistration process for plot A. However, in other plots where the accuracy of tree positioning is lower, the coregistration process was unsuccessful. In contrast, the proposed method, by reducing its dependency on tree positioning accuracy, managed to provide successful results across all datasets within a reasonable processing time.

A comparative analysis was conducted between the results of the proposed method with/without the removal of small trees in Table V. The findings indicate that removing small trees has significantly improved the computational performance of the proposed method, particularly in datasets with higher complexity. Furthermore, the accuracy of registration has demonstrated enhancement across all datasets following the elimination of small trees.

IV. Conclusion

Point cloud registration in forest environments is always considered a challenge due to the complex structure of trees and the limited presence of stable features in these environments. This article proposed an automatic and robust method for point cloud registration of TLS and ALS based on trees stem positions in forest environments. Existing tree-based registration methods heavily rely on the accuracy of trees stem localization, which can be challenging in certain forest areas with different

complexities. Therefore, an approach that is less sensitive to trees stem localization accuracy is adopted in this article. In the first step of the proposed approach, a filtering process is employed to remove small trees in the TLS data that have a low potential for accurate localization in the ALS data based on their DBH information.

On the other hand, to reduce the search space in the ALS data, a point filtering process using local triangulation is applied. In this process, local triangulations are generated for both the TLS and ALS data. For each triangular structure in the TLS data, initial triangles with similar triangular structures in the ALS data are identified. In contrast, triangles that do not have similar structures are removed from further computational processes. This filtering approach helps in reducing the search space and improving the efficiency of the point cloud registration process. Next, the proposed method utilizes an iterative approach to identify stable correspondences between the TLS and ALS data. The registration process was performed after identifying initial correspondences and estimating the transformation parameters. The proposed method was applied on different areas of TLS and ALS point clouds from forest environments with varying complexities. The obtained results demonstrated the satisfactory accuracy of the proposed point cloud registration method in dealing with complex forest structures. Moreover, the proposed method has demonstrated its effectiveness in scenarios where precise tree locations have not been determined, thereby mitigating the sensitivity to the accuracy of individual tree location extraction.

The potential of the proposed method in point cloud registration over a large search radius of ALS data was evaluated. The method successfully performs the registration process for a plot with high tree localization accuracy, covering an approximate search radius of 113 ha and containing around 60 000 tree locations. In addition, the registration process was also successfully completed for plots with lower tree localization accuracy and areas of approximately 20 to 40 ha, which included about 10 000 to 20 000 tree locations.

On the flip side, the suggested method is robust regarding rotational and translational changes between two-point cloud datasets. As a result, for practical applications, the requirement for meticulous absolute positioning is notably diminished during the collection of TLS data, especially in dense forests where the GNSS signal is weakened in close proximity to the ground.

The main focus of this article is to increase the robustness and reduce the sensitivity of point cloud registration to the accuracy of trees stem localization. As a future research direction, improving the algorithm's computing efficiency further is suggested.

ACKNOWLEDGMENT

The authors acknowledge TU Wien Bibliothek for financial support through its Open Access Funding Program.

REFERENCES

[1] T. Yang, J. Ye, S. Zhou, A. Xu, and J. Yin, "3D reconstruction method for tree seedlings based on point cloud self-registration," *Comput. Electron. Agriculture*, vol. 200, 2022, Art. no. 107210.

[2] Ö. Zováthi, B. Nagy, and C. Benedek, "Point cloud registration and change detection in urban environment using an onboard Lidar sensor and MLS reference data," *Int. J. Appl. Earth Observ. Geoinf.*, vol. 110, 2022, Art. no. 102767.

[3] H. Zhao, M. Tang, and H. Ding, "HoPPF: A novel local surface descriptor for 3D object recognition," *Pattern Recognit.*, vol. 103, 2020, Art. no. 107272.

[4] P. Kim, J. Chen, and Y. K. Cho, "SLAM-driven robotic mapping and registration of 3D point clouds," *Automat. Construction*, vol. 89, pp. 38–48, 2018.

[5] A. Zaganidis, L. Sun, T. Duckett, and G. Cielniak, "Integrating deep semantic segmentation into 3-D point cloud registration," *IEEE Robot. Automat. Lett.*, vol. 3, no. 4, pp. 2942–2949, Oct. 2018.

[6] K. D. Rocha et al., "Crown-level structure and fuel load characterization from airborne and terrestrial laser scanning in a longleaf pine (Pinus palustris Mill.) forest ecosystem," *Remote Sens.*, vol. 15, 2023, Art. no. 1002.

[7] G. Liu, J. Wang, P. Dong, Y. Chen, and Z. Liu, "Estimating individual tree height and diameter at breast height (DBH) from terrestrial laser scanning (TLS) data at plot level," *Forests*, vol. 9, 2018, Art. no. 398.

[8] L. Liu, Y. Pang, Z. Li, L. Si, and S. Liao, "Combining airborne and terrestrial laser scanning technologies to measure forest understorey volume," *Forests*, vol. 8, 2017, Art. no. 111.

[9] L. Cheng et al., "Registration of laser scanning point clouds: A review," *Sensors*, vol. 18, 2018, Art. no. 1641.

[10] J. G. Henning and P. J. Radtke, "Ground-based laser imaging for assessing three-dimensional forest canopy structure," *Photogrammetric Eng. Remote Sens.*, vol. 72, pp. 1349–1358, 2006.

[11] X. Liang and J. Hyyppä, "Automatic stem mapping by merging several terrestrial laser scans at the feature and decision levels," *Sensors*, vol. 13, pp. 1614–1634, 2013.

[12] J. Liu et al., "Automated matching of multiple terrestrial laser scans for stem mapping without the use of artificial references," *Int. J. Appl. Earth Observ. Geoinf.*, vol. 56, pp. 13–23, 2017.

[13] D. Kelbe, J. Van Aardt, P. Romanczyk, M. Van Leeuwen, and K. Cawse-Nicholson, "Marker-free registration of forest terrestrial laser scanner data pairs with embedded confidence metrics," *IEEE Trans. Geosci. Remote Sens.*, vol. 54, no. 7, pp. 4314–4330, Jul. 2016.

[14] P. Polewski, A. Erickson, W. Yao, N. Coops, P. Krzystek, and U. Stilla, "Object-based coregistration of terrestrial photogrammetric and ALS point clouds in forested areas," *ISPRS Ann. Photogrammetry Remote Sens. Spatial Inf. Sci.*, vol. 3, 2016, Art. no. 347.

[15] E. Hyyppä, J. Muhojoki, X. Yu, A. Kukko, H. Kaartinen, and J. Hyyppä, "Efficient coarse registration method using translation-and rotation-invariant local descriptors towards fully automated forest inventory," *ISPRS Open J. Photogrammetry Remote Sens.*, vol. 2, 2021, Art. no. 100007.

[16] J. Hohenthal, P. Alho, J. Hyyppä, and H. Hyyppä, "Laser scanning applications in fluvial studies," *Prog. Phys. Geogr.*, vol. 35, pp. 782–809, 2011.

[17] B. O. Abayowa, A. Yilmaz, and R. C. Hardie, "Automatic registration of optical aerial imagery to a LiDAR point cloud for generation of city models," *ISPRS J. Photogrammetry Remote Sens.*, vol. 106, pp. 68–81, 2015.

[18] L. Zhu and R. Shi, "Research on target accuracy for ground-based lidar," in *Proc. Laser Radar Technol. Appl. XIV*, 2009, pp. 134–146.

[19] M. Y. Yang, Y. Cao, and J. McDonald, "Fusion of camera images and laser scans for wide baseline 3D scene alignment in urban environments," *ISPRS J. Photogrammetry Remote Sens.*, vol. 66, pp. S52–S61, 2011.

[20] J. Avbelj, D. Iwaszczuk, R. Müller, P. Reinartz, and U. Stilla, "Coregistration refinement of hyperspectral images and DSM: An object-based approach using spectral information," *ISPRS J. Photogrammetry Remote Sens.*, vol. 100, pp. 23–34, 2015.

[21] D. Grant, J. Bethel, and M. Crawford, "Point-to-plane registration of terrestrial laser scans," *ISPRS J. Photogrammetry Remote Sens.*, vol. 72, pp. 16–26, 2012.

[22] H. Wu, X. Guan, and J. Gong, "ParaStream: A parallel streaming Delaunay triangulation algorithm for LiDAR points on multicore architectures," *Comput. Geosci.*, vol. 37, pp. 1355–1363, 2011.

[23] L. Cheng et al., "A symmetry-based method for LiDAR point registration," *IEEE J. Sel. Topics Appl. Earth Observ. Remote Sens.*, vol. 11, no. 1, pp. 285–299, Jan. 2018.

[24] G. T. Flitton, T. P. Breckon, and N. M. Bouallagu, "Object recognition using 3D SIFT in complex CT volumes," in *Proc. BMVC*, 2010, pp. 1–12.

[25] H. Chen and B. Bhanu, "3D free-form object recognition in range images using local surface patches," *Pattern Recognit. Lett.*, vol. 28, pp. 1252–1262, 2007.

[26] Y. Zhong, "Intrinsic shape signatures: A shape descriptor for 3D object recognition," in *Proc. IEEE 12th Int. Conf. Comput. Vis. workshops*, 2009, pp. 689–696.
[27] S. M. Prakhya, B. Liu, and W. Lin, "Detecting keypoint sets on 3D point clouds via histogram of normal orientations," *Pattern Recognit. Lett.*, vol. 83, pp. 42–48, 2016.
[28] F. Ghorbani, H. Ebadi, N. Pfeifer, and A. Sedaghat, "Uniform and competency-based 3D keypoint detection for coarse registration of point clouds with homogeneous structure," *Remote Sens.*, vol. 14, 2022, Art. no. 4099.
[29] R. B. Rusu, N. Blodow, and M. Beetz, "Fast point feature histograms (FPFH) for 3D registration," in *Proc. IEEE Int. Conf. Robot. Automat.*, 2009, pp. 3212–3217.
[30] F. Tombari, S. Salti, and L. Di Stefano, "Unique signatures of histograms for local surface description," in *Proc. 11th Eur. Conf. Comput. Vis.*, 2010, pp. 356–369.
[31] Y. Guo, F. Sohel, M. Bennamoun, M. Lu, and J. Wan, "Rotational projection statistics for 3D local surface description and object recognition," *Int. J. Comput. Vis.*, vol. 105, pp. 63–86, 2013.
[32] Z. Dong, B. Yang, F. Liang, R. Huang, and S. Scherer, "Hierarchical registration of unordered TLS point clouds based on binary shape context descriptor," *ISPRS J. Photogrammetry Remote Sens.*, vol. 144, pp. 61–79, 2018.
[33] F. Ghorbani, H. Ebadi, A. Sedaghat, and N. Pfeifer, "A novel 3-D local DAISY-style descriptor to reduce the effect of point displacement error in point cloud registration," *IEEE J. Sel. Topics Appl. Earth Observ. Remote Sens.*, vol. 15, pp. 2254–2273, 2022.
[34] P. Polewski and W. Yao, "Scale invariant line-based co-registration of multimodal aerial data using L1 minimization of spatial and angular deviations," *ISPRS J. Photogrammetry Remote Sens.*, vol. 152, pp. 79–93, 2019.
[35] Y. Liu, X. Zhao, Y. Jiao, X. Yang, and H. Xu, "Method for real-time reconstruction of a transmission line based on the LiDAR point cloud data of a partial line segment," *Sustain. Energy Technol. Assessments*, vol. 57, 2023, Art. no. 103180.
[36] E. Xu, Z. Xu, and K. Yang, "Using 2-lines congruent sets for coarse registration of terrestrial point clouds in urban scenes," *IEEE Trans. Geosci. Remote Sens.*, vol. 60, Nov. 2021, Art. no. 5701618.
[37] Y. Tan, Y. Shi, Y. Li, and B. Xu, "Automatic registration method of multi-source point clouds based on building facades matching in urban scenes," *Photogrammetric Eng. Remote Sens.*, vol. 88, pp. 767–782, 2022.
[38] C. Armenakis, Y. Gao, and G. Sohn, "Co-registration of aerial photogrammetric and LiDAR point clouds in urban environments using automatic plane correspondence," *Appl. Geomatics*, vol. 5, pp. 155–166, 2013.
[39] X. Ge and T. Wunderlich, "Surface-based matching of 3D point clouds with variable coordinates in source and target system," *ISPRS J. Photogrammetry Remote Sens.*, vol. 111, pp. 1–12, 2016.
[40] J.-F. Tremblay and M. Béland, "Towards operational marker-free registration of terrestrial lidar data in forests," *ISPRS J. Photogrammetry Remote Sens.*, vol. 146, pp. 430–435, 2018.
[41] W. Dai et al., "Fast registration of forest terrestrial laser scans using key points detected from crowns and stems," *Int. J. Digit. Earth*, vol. 13, pp. 1585–1603, 2020.
[42] M. Hauglin, V. Lien, E. Næsset, and T. Gobakken, "Geo-referencing forest field plots by co-registration of terrestrial and airborne laser scanning data," *Int. J. Remote Sens.*, vol. 35, pp. 3135–3149, 2014.
[43] P. Polewski, W. Yao, L. Cao, and S. Gao, "Marker-free coregistration of UAV and backpack LiDAR point clouds in forested areas," *ISPRS J. Photogrammetry Remote Sens.*, vol. 147, pp. 307–318, 2019.
[44] H. Guan et al., "A novel framework to automatically fuse multiplatform LiDAR data in forest environments based on tree locations," *IEEE Trans. Geosci. Remote Sens.*, vol. 58, no. 3, pp. 2165–2177, Mar. 2019.
[45] J. Shao et al., "Efficient co-registration of UAV and ground LiDAR forest point clouds based on canopy shapes," *Int. J. Appl. Earth Observ. Geoinf.*, vol. 114, 2022, Art. no. 103067.
[46] K. Olofsson and J. Holmgren, "Co-registration of single tree maps and data captured by a moving sensor using stem diameter weighted linking," *Silva Fennica*, vol. 56, 2022, Art. no. 10712.
[47] R. Zhou et al., "Improving estimation of tree parameters by fusing ALS and TLS point cloud data based on canopy gap shape feature points," *Drones*, vol. 7, 2023, Art. no. 524.
[48] N. J. Mitra, N. Gelfand, H. Pottmann, and L. Guibas, "Registration of point cloud data from a geometric optimization perspective," in *Proc. Eurographics/ACM SIGGRAPH Symp. Geometry Process.*, 2004, pp. 22–31.
[49] K. Kraus and N. Pfeifer, "Determination of terrain models in wooded areas with airborne laser scanner data," *ISPRS J. Photogrammetry Remote Sens.*, vol. 53, pp. 193–203, 1998.
[50] G. Sithole and G. Vosselman, "Experimental comparison of filter algorithms for bare-Earth extraction from airborne laser scanning point clouds," *ISPRS J. Photogrammetry Remote Sens.*, vol. 59, pp. 85–101, 2004.
[51] V. Moudrý, P. Klápště, M. Fogl, K. Gdulová, V. Barták, and R. Urban, "Assessment of LiDAR ground filtering algorithms for determining ground surface of non-natural terrain overgrown with forest and steppe vegetation," *Measurement*, vol. 150, 2020, Art. no. 107047.
[52] G. Bailey, Y. Li, N. McKinney, D. Yoder, W. Wright, and H. Herrero, "Comparison of ground point filtering algorithms for high-density point clouds collected by terrestrial LiDAR," *Remote Sens.*, vol. 14, 2022, Art. no. 4776.
[53] G. Kermarrec, Z. Yang, and D. Czerwonka-Schröder, "Classification of terrestrial laser scanner point clouds: A comparison of methods for landslide monitoring from mathematical surface approximation," *Remote Sens.*, vol. 14, 2022, Art. no. 5099.
[54] X. Liang et al., "International benchmarking of terrestrial laser scanning approaches for forest inventories," *ISPRS J. photogrammetry Remote Sens.*, vol. 144, pp. 137–179, 2018.
[55] N. Pfeifer, G. Mandlburger, J. Otepka, and W. Karel, "OPALS—A framework for airborne laser scanning data analysis," *Comput., Environ. Urban Syst.*, vol. 45, pp. 125–136, 2014.
[56] X. Wang et al., "GlobalMatch: Registration of forest terrestrial point clouds by global matching of relative stem positions," *ISPRS J. Photogrammetry Remote Sens.*, vol. 197, pp. 71–86, Mar. 2023.
[57] M. Hollaus and Y.-C. Chen, *SilviLaser 2021 Benchmark Dataset - Terrestrial Challenge (1.1) [Data set]*. Vienna, Austria: TU Wien, 2023, doi: 10.48436/kndye-egv02.

Fariborz Ghorbani received the B.Sc. degree in geomatics engineering from the Geomatics College, Iran National Cartographic Center, Tehran, Iran, in 2014, the M.Sc. degree in photogrammetry engineering from the K. N. Toosi University of Technology, Tehran, Iran, in 2017, and the Ph.D. degree in photogrammetry and remote sensing from the K. N. Toosi University of Technology, Tehran, Iran, in 2022.

He is currently with the Photogrammetry Research Unit, Vienna University of Technology. His research interests include, point clouds processing, point cloud registration, 3-D monitoring, 3-D change detection, data fusion, images processing, feature extraction, machine learning, classification and segmentation, and UAV photogrammetry.

Yi-Chen Chen received the B.Sc. degree in geomatics and computer science, and the M.Sc. degree in geomatics from the National Cheng Kung University (NCKU), Tainan, Taiwan, in 2014 and 2016, respectively. He is currently working toward the Ph.D. degree in photogrammetry research unit with the Vienna University of Technology, Vienna, Austria.

From 2017 to 2021, he was a Research Assistant with the NCKU and industries, and worked with satellite image processing, UAV remote sensing, and machine learning. His research interests include airborne and terrestrial laser scanning, point cloud 3-D modeling, image processing, machine learning, and data fusion.

Markus Hollaus received the M.Sc. degree from the University of Natural Resources and Life Sciences (BOKU), Vienna, Austria, in 2000, and the Ph.D. degree from the Vienna University of Technology, Vienna, Austria, in 2006.

From 2001 to 2003 he was a Research Scientist with the BOKU. From 2004 to 2008, he was a Research Scientist and from 2009 to 2013 University Assistant, and since 2014 he is a Senior Scientist with the Department of Geodesy and Geoinformation at the Vienna University of Technology. His research interests focus on the derivation of vegetation parameters from LiDAR data as well as LiDAR data combined with other EO data.

Norbert Pfeifer was born in Vienna, Austria, in 1971. He received the Dipl. Ing. and Ph.D. degrees in surveying engineering from the Technische Universität Wien (TU Wien), Vienna, Austria, in 1997 and 2002, respectively.

From 2003 to 2006, he was a Research Assistant and an Assistant Professor with the TU Delft, Delft, The Netherlands. In 2006, he was a Lecturer with the Department of Geography, the University of Innsbruck, Innsbruck, Austria, and a Senior Researcher with the Centre for Natural Hazard Management, alp-S, in Innsbruck. Later in 2006, he took the position of a Professor with the TU Wien in photogrammetry. He has coauthored more than 100 articles in journals and 6 books. His research interests include LiDAR signal processing, calibration of airborne and terrestrial laser scanning, classification and segmentation of LiDAR point clouds, 3-D modeling, and application of point clouds in the environmental sciences.

Dr. Pfeifer is a member of the International Society of Photogrammetry and Remote Sensing.